Research paper

Struct Multidisc Optim 27, 210–217 (2004)
DOI 10.1007/s00158-003-0372-x

Solution to boundary shape optimization problem of linear elastic continua with prescribed natural vibration mode shapes

A.R. Inzarulfaisham and H. Azegami

Abstract This paper presents a practical method of numerical analysis for boundary shape optimization problems of linear elastic continua in which natural vibration modes approach prescribed modes on specified subboundaries. The shape gradient for the boundary shape optimization problem is evaluated with optimality conditions obtained by the adjoint variable method, the Lagrange multiplier method, and the formula for the material derivative. Reshaping is accomplished by the traction method, which has been proposed as a solution to boundary shape optimization problems of domains in which boundary value problems of partial differential equations are defined. The validity of the presented method is confirmed by numerical results of three-dimensional beam-like and plate-like continua.

Key words shape optimization, FEM, natural vibration mode, modal analysis, adjoint method

1 Introduction

The use of modal analysis is expanding rapidly, with one notable example being the widespread application of the method to investigating the structural dynamics characteristics of mechanical systems. The modal pairs consist of natural frequencies and mode shapes obtained from modal analysis are used to identify the cause of vibrational problems. By making use of the modal pairs, one can evaluate the change of dynamic properties when mass and/or stiffness is added or subtracted without changing the structure.

However, designing a mechanical system or structure with desired natural frequencies and/or mode shapes is not easy. With respect to parametric structural optimization problems, many techniques have been proposed for modal sensitivity analysis of structural systems, among them the methods reported by Fox and Kapoor (1968), Nelson (1976), Wang (1991), Hagiwara and Ma (1994), and Lin and Lim (1995). In non-parametric structural optimization problems, a technique for topology optimization of linear elastic continua based on homogenization theory was presented by Bendsoe and Kikuchi (1988) and has been applied to topology and shape optimization problems of vibrating structures by Diaz and Kikuchi (1992), Ma *et al.* (1994), and Tenek and Hagiwara (1994). In this technique, the material distribution is formulated with parameters in periodic microstructures.

A limited number of papers have been presented on non-parametric boundary shape optimization problems of linear elastic continua formulated in terms of domain perturbations from a family of one-to-one mappings. One of the authors (Azegami *et al.* 1995, 1997; Azegami and Wu 1996; Shimoda *et al.* 1998; Azegami 2000) has proposed a numerical method called the traction method, based on the gradient method in a Hilbert space, for solving boundary shape optimization problems of domains in which boundary value problems of partial differential equations are defined. Wu and Azegami (1995a,b) applied the traction method to maximizing problems of natural frequencies under a volume constraint, and to the dual problems. Wu and Azegami (1995c) and Wu *et al.* (1997, 1999, 2000) demonstrated a numerical analysis using the traction method for the minimization of frequency responses such as the strain energy, kinetic energy, and absolute mean compliance.

Received: 2 August 2002
Revised manuscript received: 6 November 2003
Published online: 23 March 2004

A.R. Inzarulfaisham[1] and H. Azegami[2, ✉]

[1] Doctoral Course, Graduate School of Mechanical and Structural System Engineering, Toyohashi University of Technology, 1-1 Hibarigaoka, Tempaku-cho, Toyohashi City, Aichi Prefecture 441-8580, Japan
e-mail: inzarul@az.mech.tut.ac.jp
[2] Department of Complex Systems Science, Graduate School of Information Science, Nagoya University, Furo-cho, Chigusa-ku, Nagoya City, Aichi Prefecture 464-8601, Japan
e-mail: azegami@is.nagoya-u.ac.jp

With the traction method, the shape sensitivity, called the shape gradient, of the given problem is evaluated by using the finite element method or boundary element method based on the optimality conditions obtained by the adjoint variable method, the Lagrange multiplier method, and the formula for the material derivative. The traction method was proposed as a procedure for determining the velocity of the domain perturbation by solving a displacement of a pseudo-elastic body defined in the domain by the loading of a pseudo-external force proportional to the negative value of the shape gradient under constraints on the displacement of the invariable boundaries. Since the traction method is implemented by using the finite element method or boundary element method, it is exceptionally easy to perform, and offers the advantage that it is not necessary to refine the mesh of the internal nodes of the domain.

This paper is concerned with a method of solving boundary shape optimization problems of linear elastic continua that have prescribed natural vibration mode shapes on specified sub-boundaries. A minimization problem of an integral of the squared error of an assigned natural vibration mode shape from a prescribed mode shape on a specified sub-boundary with respect to perturbation of the domain of the linear elastic continuum is formulated first. The shape gradient of the formulated problem is found by the adjoint variable method and the Lagrange multiplier method using the formula of the material derivative. Using the shape gradient, a procedure to analyze the domain variation with the traction method is presented.

2
Shape optimization problem with prescribed natural vibration mode shapes

Let a linear elastic continuum be defined in a three-dimensional domain $\Omega \subset \mathbb{R}^3$ and on its boundary Γ. The continuum is fixed on the sub-boundary $\Gamma_0 \subset \Gamma$, if necessary. The weak form of the governing equation for the r-th natural vibration eigenvalue $\lambda^{[r]}$ defined by the square of the r-th natural frequency and the natural vibration mode $\mathbf{u}^{[r]} \equiv \{u_i{}^{[r]}\}_{i=1,2,3} : \Omega \mapsto \mathbb{R}^3$ is represented by

$$a\left(\mathbf{u}^{[r]}, \mathbf{v}\right) = \lambda^{[r]} b\left(\mathbf{u}^{[r]}, \mathbf{v}\right), \quad \mathbf{u}^{[r]} \in U, \quad \forall \mathbf{v} \in U, \tag{1}$$

where the bilinear forms $a(\,\cdot\,,\,\cdot\,)$ and $b(\,\cdot\,,\,\cdot\,)$ and the admissible functional space U are defined by

$$a(\mathbf{u}, \mathbf{v}) \equiv \int_{\Omega} C_{ijkl} u_{k,l} v_{i,j} \, \mathrm{d}x, \quad \mathbf{u}, \mathbf{v} \in U, \tag{2}$$

$$b(\mathbf{u}, \mathbf{v}) \equiv \int_{\Omega} \rho u_i v_i \, \mathrm{d}x, \quad \mathbf{u}, \mathbf{v} \in U, \tag{3}$$

$$U \equiv \left\{ \mathbf{v} \in \left(H^1(\Omega)\right)^3 \,\middle|\, \mathbf{v}|_{\Gamma_0} = \mathbf{0},\ \Gamma_0 \subset \Gamma \right\}. \tag{4}$$

The symbols $\{C_{ijkl}\}_{i,j,k,l=1,2,3}$ and ρ are the stiffness of the linear elastic material and the density respectively. In this paper, we use the summation convention and the notation $(\,\cdot\,)_{,i} = \partial(\,\cdot\,)/\partial x_i$ for the partial differential, where $\{x_i\}_{i=1,2,3}$ is a coordinate system in $\mathbb{R}^3$. The symbol $H^m(\Omega)$ denotes Sobolev space of square integrable, until m-order derivatives, functions defined in Ω.

Domain perturbation of Ω to $\Omega_s \subset \mathbb{R}^3$ can be represented by using a one-parameter family of one-to-one mappings as presented by Zolésio (1981), Pironneau (1984), and Sokolowski and Zolésio (1991):

$$\mathbf{T}_s \equiv \{T_{si}\}_{i=1,2,3} : \Omega \ni \mathbf{X} \mapsto \mathbf{x} \in \Omega_s, \quad 0 \le s < \epsilon, \tag{5}$$

$$\mathbf{T}_s^{-1} \equiv \{T_{si}^{-1}\}_{i=1,2,3} : \Omega_s \ni \mathbf{x} \mapsto \mathbf{X} \in \Omega, \tag{6}$$

where ϵ is a small positive number. The derivative of $\mathbf{T}_s$ with respect to s defined by

$$\mathbf{V}(\mathbf{x}) \equiv \frac{\partial \mathbf{T}_s}{\partial s}\left(\mathbf{T}_s^{-1}(\mathbf{x})\right), \quad \mathbf{x} \in \Omega_s, \tag{7}$$

is called the velocity.

Using the definitions above, the shape optimization problem in which the assigned r-th natural vibration mode shape $\mathbf{u}^{[r]}$ approaches the prescribed mode $\bar{\mathbf{u}}^{[r]}$ on the specified sub-boundary $\Gamma_D \subset \Gamma \setminus \Gamma_0$ while the natural vibration eigenvalue is constrained to be greater than $\bar{\lambda}^{[r]}$ and the volume is constrained to be less than $\bar{M}$ can be formulated as the minimization problem of the squared error integral $E(\alpha\mathbf{u}^{[r]} - \bar{\mathbf{u}}^{[r]}, \alpha\mathbf{u}^{[r]} - \bar{\mathbf{u}}^{[r]})$ for all modal scaling factors $\alpha \in \mathbb{R}$ by using the definition of the bilinear form $E(\,\cdot\,,\,\cdot\,)$,

$$E(\mathbf{u}, \mathbf{v}) \equiv \int_{\Gamma_D} u_i v_i \, \mathrm{d}x. \tag{8}$$

This problem can be described by

$$\min_{\Omega \subset \mathbb{R}^3, \mathbf{u}^{[r]} \in U, \alpha \in \mathbb{R}} E\left(\alpha\mathbf{u}^{[r]} - \bar{\mathbf{u}}^{[r]}, \alpha\mathbf{u}^{[r]} - \bar{\mathbf{u}}^{[r]}\right)$$

$$\text{such that (1)}, \ \lambda^{[r]} \ge \bar{\lambda}^{[r]}, \ \text{and} \ \int_{\Omega} \mathrm{d}x \le \bar{M}. \tag{9}$$

The order in which the natural vibration modes are called should be defined, because the order can change in the process of shape change. In this paper, the order is defined at the initial shape and does not depend on the actual order based on the magnitude in the process of shape change. Determining the correspondence of the assigned natural vibration mode to the renewed mode during shape change and identifying the assigned natural vibration mode from natural vibration modes with multiple natural vibration eigenvalues can be done with the MAC (Modal Assurance Criteria), a technique for estimating the degree of correlation between mode shapes (see Allemang and Brown (1982)).

3
Shape gradient

To solve problem (9) by the traction method, it is necessary to evaluate the shape gradient of the problem. The standard procedure for deriving the theoretical relations to calculate the shape gradient is to apply the adjoint variable method and the Lagrange multiplier method. The Lagrange multiplier form of the problem, $L(\mathbf{u}^{[r]}, \mathbf{v}, \mathit{\Lambda}_1, \mathit{\Lambda}_2)$, is defined by

$$L \equiv E\left(\alpha\mathbf{u}^{[r]} - \bar{\mathbf{u}}^{[r]}, \alpha\mathbf{u}^{[r]} - \bar{\mathbf{u}}^{[r]}\right) - a\left(\mathbf{u}^{[r]}, \mathbf{v}\right) + \lambda^{[r]} b\left(\mathbf{u}^{[r]}, \mathbf{v}\right) - \mathit{\Lambda}_1\left(\lambda^{[r]} - \bar{\lambda}^{[r]}\right) + \mathit{\Lambda}_2\left(\int_{\Omega} \mathrm{d}x - \bar{M}\right), \tag{10}$$

where $\mathbf{v} \equiv \{v_i\}_{i=1,2,3} \in U$ has been introduced as the adjoint variable with respect to the weak form (1). In this paper, we call $\mathbf{v}$ the adjoint mode. $\mathit{\Lambda}_1$ and $\mathit{\Lambda}_2$ have been introduced as the Lagrange multipliers with respect to the natural vibration eigenvalue constraint and the volume constraint in (9) respectively.

For the sake of simplicity, let $\{C_{ijkl}\}_{i,j,k,l=1,2,3}$ and ρ be fixed in $\mathbb{R}^3$ and let the sub-boundary $\mathit{\Gamma}_0 \cup \mathit{\Gamma}_D$ be invariable during domain perturbations. By using the formula of the material derivative as shown in Sokolowski and Zolésio (1991), the shape derivative of the Lagrange functional $\dot{L} \equiv \mathrm{d}L/\mathrm{d}s$ is obtained by

$$\dot{L} = 2\alpha E\left(\alpha\mathbf{u}^{[r]} - \bar{\mathbf{u}}^{[r]}, \mathbf{u}^{[r]\prime}\right) + 2\dot{\alpha}E\left(\alpha\mathbf{u}^{[r]} - \bar{\mathbf{u}}^{[r]}, \mathbf{u}^{[r]}\right) - a\left(\mathbf{u}^{[r]\prime}, \mathbf{v}\right) - a\left(\mathbf{u}^{[r]}, \mathbf{v}'\right) + \lambda^{[r]} b\left(\mathbf{u}^{[r]\prime}, \mathbf{v}\right) + \lambda^{[r]} b\left(\mathbf{u}^{[r]}, \mathbf{v}'\right) + \dot{\lambda}^{[r]} b\left(\mathbf{u}^{[r]}, \mathbf{v}\right) - \dot{\mathit{\Lambda}}_1\left(\lambda^{[r]} - \bar{\lambda}^{[r]}\right) - \dot{\lambda}^{[r]}\mathit{\Lambda}_1 + \dot{\mathit{\Lambda}}_2\left(\int_{\Omega} \mathrm{d}x - \bar{M}\right) + \langle G\boldsymbol{\nu}, \mathbf{V}\rangle, \tag{11}$$

where the linear form $\langle G\boldsymbol{\nu}, \mathbf{V}\rangle$ with respect to the velocity $\mathbf{V}$ is defined by

$$\langle G\boldsymbol{\nu}, \mathbf{V}\rangle \equiv \int_{\mathit{\Gamma}} G\nu_i V_i \,\mathrm{d}\mathit{\Gamma}, \tag{12}$$

$$G = -C_{ijkl} u^{[r]}_{k,l} v_{i,j} + \rho\lambda^{[r]} u^{[r]}_i v_i + \mathit{\Lambda}_2 . \tag{13}$$

The notation $(\cdot)'$ represents the derivative of a function $(\cdot)$ with respect to domain perturbation expressed with the fixed spatial coordinates that is called the shape derivative in Sokolowski and Zolésio (1991). The symbol $\boldsymbol{\nu} \equiv \{\nu_i\}_{i=1,2,3} : \mathit{\Gamma} \mapsto \mathbb{R}^3$ denotes the outer normal vector.

Considering the stationary conditions for all $\mathbf{u}^{[r]\prime} \in U$, $\mathbf{v}' \in U$, $\dot{\alpha} \in \mathbb{R}$, $\dot{\mathit{\Lambda}}_1 \in \mathbb{R}$, and $\dot{\mathit{\Lambda}}_2 \in \mathbb{R}$, the Kuhn–Tucker conditions with respect to $\mathbf{u}^{[r]}$, $\mathbf{v}$, α, $\mathit{\Lambda}_1$, and $\mathit{\Lambda}_2$ are obtained as

$$a\left(\mathbf{u}^{[r]}, \mathbf{v}'\right) = \lambda^{[r]} b\left(\mathbf{u}^{[r]}, \mathbf{v}'\right), \quad \forall\mathbf{v}' \in U, \tag{14}$$

$$\alpha E\left(\mathbf{u}^{[r]}, \mathbf{u}^{[r]}\right) = E\left(\bar{\mathbf{u}}^{[r]}, \mathbf{u}^{[r]}\right), \tag{15}$$

$$a\left(\mathbf{v}, \mathbf{u}'^{[r]}\right) = \lambda^{[r]} b\left(\mathbf{v}, \mathbf{u}^{[r]\prime}\right) + 2\alpha E\left(\alpha\mathbf{u}^{[r]} - \bar{\mathbf{u}}^{[r]}, \mathbf{u}^{[r]\prime}\right), \quad \forall\mathbf{u}^{[r]\prime} \in U, \tag{16}$$

$$b\left(\mathbf{u}^{[r]}, \mathbf{v}\right) = \mathit{\Lambda}_1, \quad \forall\mathbf{v} \in U, \tag{17}$$

$$\mathit{\Lambda}_1 \geq 0, \quad \lambda^{[r]} \geq \bar{\lambda}^{[r]}, \quad \mathit{\Lambda}_1\left(\lambda^{[r]} - \bar{\lambda}^{[r]}\right) = 0, \tag{18}$$

$$\mathit{\Lambda}_2 \geq 0, \quad \int_{\Omega} \mathrm{d}x \leq \bar{M}, \quad \mathit{\Lambda}_2\left(\int_{\Omega} \mathrm{d}x - \bar{M}\right) = 0 \tag{19}$$

When $\mathbf{u}^{[r]}$ is determined by (1), (14) can be satisfied. (15) gives the governing equation for $\alpha \in \mathbb{R}$. (16) gives the governing equation for the adjoint mode $\mathbf{v} \in U$ and is called the adjoint equation of the shape optimization problem. The solution to the adjoint equation will be presented in the next section. The inequalities (18) and (19) give the governing equations for $\mathit{\Lambda}_1$ and $\mathit{\Lambda}_2$ respectively. Based on the duality theorem, the optimum solution of $\mathit{\Lambda}_1$ and $\mathit{\Lambda}_2$ can be determined as the positive values that maximize the Lagrange multiplier form. These maximum conditions give a way of finding the optimum values for $\mathit{\Lambda}_1$ and $\mathit{\Lambda}_2$ by increasing the Lagrange multipliers $\mathit{\Lambda}_1$ and $\mathit{\Lambda}_2$ when these inequality equations are not satisfied in well-suited problems.

When $\mathbf{u}^{[r]}$, $\mathbf{v}$, α, $\mathit{\Lambda}_1$, and $\mathit{\Lambda}_2$ are determined by (14)–(19), the derivative of the Lagrange multiplier form agrees with the derivative of the objective functional because all the constraints are satisfied. It is given by the linear form $\langle G\boldsymbol{\nu}, \mathbf{V}\rangle$ with respect to $\mathbf{V}$:

$$\dot{L}\Big|_{\mathbf{u}^{[r]},\mathbf{v},\alpha,\mathit{\Lambda}_1,\mathit{\Lambda}_2} = \dot{E}\left(\alpha\mathbf{u}^{[r]} - \bar{\mathbf{u}}^{[r]}, \alpha\mathbf{u}^{[r]} - \bar{\mathbf{u}}^{[r]}\right)\Big|_{\mathbf{u}^{[r]},\mathbf{v},\alpha,\mathit{\Lambda}_1,\mathit{\Lambda}_2} = \langle G\boldsymbol{\nu}, \mathbf{V}\rangle . \tag{20}$$

From the fact that the function $G\boldsymbol{\nu}$ is a coefficient function with respect to the velocity $\mathbf{V}$, which is the derivative of the design variable $\mathbf{T}_s$, $G\boldsymbol{\nu}$ indicates a sensitivity of this problem, which we call the shape gradient. In particular, the function G is called the shape gradient density of the problem.

4
Solution to adjoint equation

The Kuhn–Tucker conditions with respect to the adjoint mode $\mathbf{v} \in U$ are given by (16) and (17). In this paper,

an approach using the modal coordinate system will be considered in which the adjoint mode $\mathbf{v}$ can be expressed by superposing the mode shapes with adjoint modal variables $\{\xi^{[p]}\}_{p=1}^{N}$ of finite number N. Considering the orthogonality with $b(\,\cdot\,,\,\cdot\,)$ among $\{\mathbf{u}^{[p]}\}_{p=1}^{N}$ in (17), it is convenient to divide $\mathbf{v}$ into ${}^0\mathbf{v}$ for $p \neq r$ and ${}^1\mathbf{v}$ for $p = r$:

$$\mathbf{v} = {}^0\mathbf{v} + {}^1\mathbf{v}\,, \tag{21}$$

$${}^0\mathbf{v} = \sum_{p=1,2,\cdots,N,\ p\neq r} \mathbf{u}^{[p]}\xi^{[p]}\,, \tag{22}$$

$${}^1\mathbf{v} = \mathbf{u}^{[r]}\xi^{[r]}\,. \tag{23}$$

Substituting (22) into $\mathbf{v}$ in (16), assuming $\mathbf{u}^{[r]\prime} = \mathbf{u}^{[p]}$, and considering the p-th natural vibration equations such as (1), the adjoint modal variables $\{\xi^{[p]}\}_{p=1,2,\cdots,N,\ p\neq r}$ are calculated by

$$\xi^{[p]} = \frac{2\alpha E\left(\alpha\mathbf{u}^{[r]} - \bar{\mathbf{u}}^{[r]}, \mathbf{u}^{[p]}\right)}{\left(\lambda^{[p]} - \lambda^{[r]}\right) b\left(\mathbf{u}^{[p]}, \mathbf{u}^{[p]}\right)}\,. \tag{24}$$

On the other hand, substituting (21) into $\mathbf{v}$ in (17) and considering the orthogonality among $\{\mathbf{u}^{[p]}\}_{p=1}^{N}$, $\xi^{[r]}$ is equal to Λ_1.

Therefore, the adjoint mode $\mathbf{v}$ can be evaluated with the natural vibration eigenvalues $\{\lambda^{[p]}\}_{p=1}^{N}$ and the adjoint modal variables $\{\xi^{[p]}\}_{p=1}^{N}$ as

$$\mathbf{v} = \sum_{p=1,2,\cdots,N,\ p\neq r} \frac{2\alpha E\left(\alpha\mathbf{u}^{[r]} - \bar{\mathbf{u}}^{[r]}, \mathbf{u}^{[p]}\right)}{\left(\lambda^{[p]} - \lambda^{[r]}\right) b\left(\mathbf{u}^{[p]}, \mathbf{u}^{[p]}\right)}\mathbf{u}^{[p]} + \mathbf{u}^{[r]}\Lambda_1\,. \tag{25}$$

For determining the number of mode shapes N, it can be a practical estimation to examine the asymptotic convergence of the solution for $\mathbf{v}$ with respect to increasing N that includes higher mode shapes similar in deformation type to the assigned r-th natural vibration mode shape, such as transverse bending, lateral bending, or twisting.

5 Traction method

When the shape gradient is evaluated, the traction method can be employed for reshaping. The traction method has been proposed as an iteration procedure of the following steps when the shape gradient density is given by $G = G_0 + \sum_{m=1}^{M}\Lambda_m G_m$:

(i) Solving the state equations and the adjoint equations and evaluating the objective and constraint functionals and $\{G_m\}_{m=0}^{M}$

(ii) Solving the velocity $\{\mathbf{V}_m\}_{m=0}^{M}$, $\mathbf{V}_m \in D$ using $\{G_m\}_{m=0}^{M}$ by

$$a(\mathbf{V}_m, \mathbf{y}) = -\langle G_m\boldsymbol{\nu}, \mathbf{y}\rangle\,, \quad \forall\mathbf{y} \in D\,, \tag{26}$$

where $a(\,\cdot\,,\,\cdot\,)$ is defined by (2) and

$$D \equiv \left\{\, \mathbf{V} \in \left(H^1(\Omega)\right)^3 \,\middle|\, \mathbf{V}|_{\Gamma_0\cup\Gamma_D} = 0 \,\right\} \tag{27}$$

(iii) Determining the Lagrange multipliers $\{\Lambda_m\}_{m=1}^{M}$ that satisfy the Kuhn–Tucker conditions by using the Newton–Raphson method, for example

(iv) Reshaping Ω by the mapping $\mathbf{I} + s\mathbf{V} : \Omega \mapsto \Omega_s$, where $\mathbf{V} = (\mathbf{V}_0 + \sum_{m=1}^{M}\Lambda_m\mathbf{V}_m)$, $\mathbf{I}$ is the identity mapping, and s is an incremental parameter, then returning to (i) and judging convergence at (i)

(26) indicates that the velocity $\mathbf{V}_m$ is obtained as a displacement of a pseudo-elastic body defined in Ω by the loading of a pseudo-external force of $-G_m\boldsymbol{\nu}$ under restriction on $\Gamma_0 \cup \Gamma_D$ as defined in (27), which was assumed in the derivation of the material derivative of the Lagrange multiplier in (11). That the velocity $\mathbf{V}$ decreases the objective functional can be confirmed with the coerciveness of the bilinear form $a(\,\cdot\,,\,\cdot\,)$ in a Hilbert space of D:

$$\exists\beta,\gamma > 0 :\ a(\mathbf{V},\mathbf{V}) \geq \beta\|\mathbf{V}\|_D^2 \quad \forall\mathbf{V} \in D \quad \text{and}$$
$$a(\mathbf{V},\mathbf{y}) \leq \gamma\|\mathbf{V}\|_D\|\mathbf{y}\|_D \quad \forall\mathbf{V},\mathbf{y} \in D \tag{28}$$

When the objective functionals at Ω and Ω_s are expressed by $E(\alpha\mathbf{u}^{[r]} - \bar{\mathbf{u}}^{[r]}, \alpha\mathbf{u}^{[r]} - \bar{\mathbf{u}}^{[r]})\big|_{\Omega}$ and $E(\alpha\mathbf{u}^{[r]} - \bar{\mathbf{u}}^{[r]}, \alpha\mathbf{u}^{[r]} - \bar{\mathbf{u}}^{[r]})\big|_{\Omega_s}$, using the coerciveness of $a(\,\cdot\,,\,\cdot\,)$ in (28), the following relation holds:

$$\begin{aligned}
&E\left(\alpha\mathbf{u}^{[r]} - \bar{\mathbf{u}}^{[r]}, \alpha\mathbf{u}^{[r]} - \bar{\mathbf{u}}^{[r]}\right)\Big|_{\Omega_s} = \\
&E\left(\alpha\mathbf{u}^{[r]} - \bar{\mathbf{u}}^{[r]}, \alpha\mathbf{u}^{[r]} - \bar{\mathbf{u}}^{[r]}\right)\Big|_{\Omega} + \langle G\boldsymbol{\nu}, s\mathbf{V}\rangle + o(s) = \\
&E\left(\alpha\mathbf{u}^{[r]} - \bar{\mathbf{u}}^{[r]}, \alpha\mathbf{u}^{[r]} - \bar{\mathbf{u}}^{[r]}\right)\Big|_{\Omega} - a(\mathbf{V}, s\mathbf{V}) + o(s) \leq \\
&E(\alpha\mathbf{u}^{[r]} - \bar{\mathbf{u}}^{[r]}, \alpha\mathbf{u}^{[r]} - \bar{\mathbf{u}}^{[r]})\Big|_{\Omega} - \beta s\|\mathbf{V}\|_D^2 + o(s)\,,
\end{aligned} \tag{29}$$

where $o(\cdot)$ is the Landau functional, i.e. $\lim_{s\to 0}\frac{1}{s}o(s) = 0$. Indeed, the second term on the right side of the inequality is strictly negative and the third term can be made very small. The robustness of the traction method against oscillating phenomena, which often occur in moving the boundary nodes of finite element models in proportion to the negative value of the shape gradient, has been confirmed theoretically in a previous paper by Azegami *et al.* (1997).

6 Numerical examples

The presented algorithm was implemented in a computer program that analyzes, by using the finite element method, optimum shapes of linear elastic continua that have prescribed natural vibration mode shapes on specified sub-boundaries. By using the program, numerical analyses of a beam-like three-dimensional continuum

clamped at one end and a three-dimensional free supported plate-like continuum were conducted.

The finite element models were constructed using commercial software (MSC.Patran). The modal analyses of the models were performed using commercial software (MSC.Nastran) for the beam-like continuum model and a original program that used the Lanczos method and spectral conversion for the plate-like continuum model. The validity of the original program was confirmed by agreement with the numerical results of the commercial software (MSC.Nastran).

To identify the assigned natural vibration mode on the renewed model, the MAC was employed. Using the notation $\Omega^{(k-1)}$, $b(\,\cdot\,,\,\cdot\,)|_{\Omega^{(k-1)}}$, and $\{\mathbf{u}^{[p](k-1)}\}_{p=1}^{N}$ for the domain in the previous step, the bilinear form in $\Omega^{(k-1)}$, and the natural vibration modes normalized with $b(\mathbf{u}^{[p](k-1)},\ \mathbf{u}^{[p](k-1)})\big|_{\Omega^{(k-1)}} = 1$ and $\Omega^{(k)}$, $b(\,\cdot\,,\,\cdot\,)|_{\Omega^{(k)}}$, and $\{\mathbf{u}^{[p](k)}\}_{p=1}^{N}$ for those of the renewed model, we evaluated $b(\mathbf{u}^{[r](k-1)},\ \mathbf{u}^{[p](k)})\big|_{\Omega^{(k)}}$ for all the normal mode shapes $\{\mathbf{u}^{[p](k)}\}_{p=1}^{N}$ and chose the natural vibration mode $\mathbf{u}^{[q](k)}$ that had a value nearest to 1 in $b(\mathbf{u}^{[r](k-1)}, \mathbf{u}^{[q](k)})\big|_{\Omega^{(k)}}$ as the assigned natural vibration mode in the renewed model.

The number of mode shapes, N, used in the evaluation of the adjoint modes was determined by examining the asymptotic convergence of the solution for the adjoint modes with respect to increasing N before the optimization analyses. From the examinations, $N = 10$ and 15 were selected for the beam-like continuum and the plate-like continuum respectively.

6.1
Beam-like continuum problem

Figure 1 illustrates the shapes of the finite element models of the beam-like continuum, which was assumed to be completely fixed on the front plane boundary and fixed in the normal direction on the bottom plane boundary, i.e.

$$U = \Big\{\ \mathbf{v} \in \big(H^1(\Omega)\big)^3 \Big|\ \mathbf{v}|_{\{\mathbf{x}\in\Gamma|x_3=0\}} = \mathbf{0}\,,\quad v_2|_{\{\mathbf{x}\in\Gamma|x_2=0\}} = 0 \Big\}\,. \tag{30}$$

The prescribed natural vibration mode $\bar{\mathbf{u}}^{[r]}$ was given with the first natural vibration mode on the bottom plane boundary in the reference model shown in Fig. 1a, i.e.

$$\Gamma_D = \{\mathbf{x} \in \Gamma|\ x_2 = 0\}\,, \tag{31}$$

$$\bar{\mathbf{u}}^{[r]} = \Big\{\ u_1^{[1]} \in H^{1/2}(\Gamma_D) \Big|\ u_1^{[1]} \text{ at Fig. 1a} \Big\}\,. \tag{32}$$

In the analysis of domain variation by the traction method, the front and bottom plane boundaries were completely fixed and all the side plane boundaries were fixed in the normal direction, i.e.

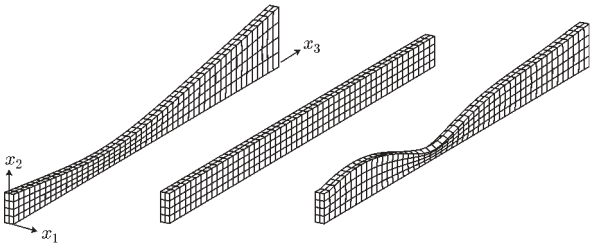

(a) Reference (b) Initial (c) Optimal

Fig. 1 Beam-like continuum problem: shape optimization of three-dimensional beam-like continuum clamped on the front plane in which the first natural vibration mode on the bottom plane, $\mathbf{u}^{[1]}$, approaches the first natural vibration mode on the bottom plane, $\bar{\mathbf{u}}^{[1]}$, of the reference beam-like continuum shown in (a)

$$D = \Big\{\ \mathbf{V} \in \big(H^1(\Omega)\big)^3 \Big|\ \mathbf{V}|_{\{\mathbf{x}\in\Gamma|x_3=0\}\cup\{\mathbf{x}\in\Gamma|x_2=0\}} = \mathbf{0}\,,\ \text{fixing normal direction on all the side plane} \Big\}\,. \tag{33}$$

The lower limit of the first natural vibration eigenvalue $\bar{\lambda}^{[1]}$ and the upper limit of the volume $\bar{M}$ were chosen as $\lambda^{[1]}$ and $\int_\Omega \mathrm{d}x$ for the reference model shown in Fig. 1a. Starting from the initial model shown in Fig. 1b, the convergent optimal model was obtained as shown in Fig. 1c.

Figure 2 illustrates the iteration history of the objective functional of the squared error integral $E(\alpha\mathbf{u}^{[1]} - \bar{\mathbf{u}}^{[1]}, \alpha\mathbf{u}^{[1]} - \bar{\mathbf{u}}^{[1]})$, the first natural vibration eigenvalue $\lambda^{[1]}$, and the volume $\int_\Omega \mathrm{d}x$, which were successfully converged to the optimal condition satisfying the inequality constraints on $\lambda^{[1]}$ and $\int_\Omega \mathrm{d}x$. A comparison of the first natural vibration modes $\alpha\mathbf{u}^{[1]}$ of the reference, initial, and optimal beam-like continua with the optimal α determined by (15) on the center line in the bottom plane boundary is illustrated in Fig. 3. From the results, it can be confirmed that the first natural vibration mode approached the prescribed mode uniformly. Figures 4 and 5

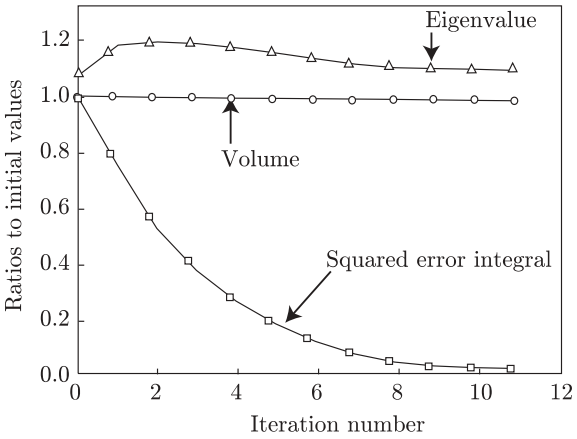

Fig. 2 Beam-like continuum problem: iteration history of the objective functional of the squared error integral $E(\alpha\mathbf{u}^{[1]} - \bar{\mathbf{u}}^{[1]}, \alpha\mathbf{u}^{[1]} - \bar{\mathbf{u}}^{[1]})$, the first natural vibration eigenvalue $\lambda^{[1]}$, and the volume $\int_\Omega \mathrm{d}x$

show comparisons of the second and third natural vibration modes obtained as the results of the prescribed first natural vibration mode shape problem. From the results of Figs. 4 and 5, it can be said that not only the first natural vibration mode, but also the higher natural vibration modes, approached those of the reference beam-like continuum in this problem.

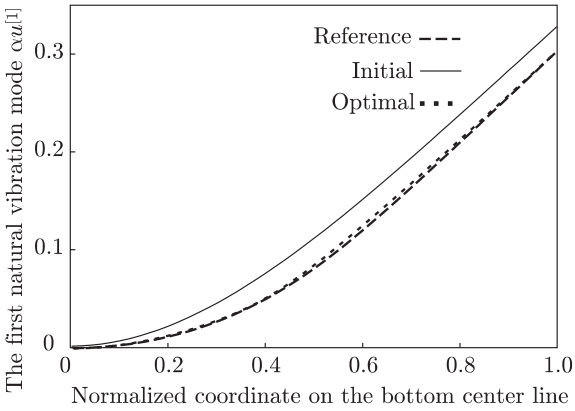

Fig. 3 Beam-like continuum problem: comparisons of the first natural vibration modes $\alpha \mathbf{u}^{[1]}$ of the reference, initial, and optimal beam-like continua with the optimal α determined by (15) on the center line in the bottom plane

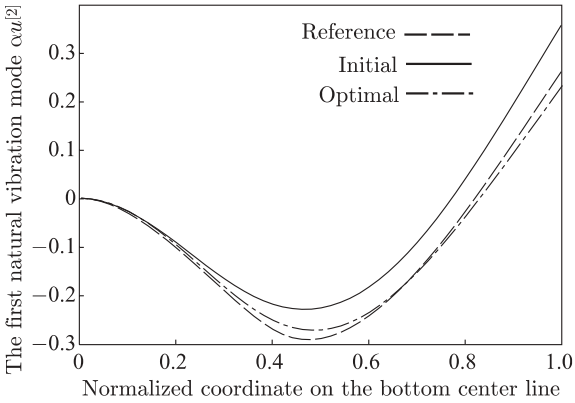

Fig. 4 Beam-like continuum problem: comparisons of the second natural vibration modes $\alpha \mathbf{u}^{[2]}$ of the reference, initial, and optimal beam-like continua with the optimal α determined by (15) on the center line in the bottom plane

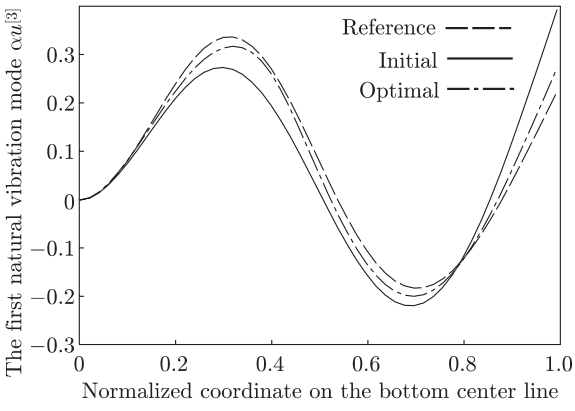

Fig. 5 Beam-like continuum problem: comparisons of the third natural vibration modes $\alpha \mathbf{u}^{[3]}$ of the reference, initial, and optimal beam-like continua with the optimal α determined by (15) on the center line in the bottom plane

6.2 Plate-like continuum problem

As a supported free continuum problem in which rigid body modes should be taken into account, the plate-like continuum problem shown in Fig. 6 was analyzed. The prescribed natural vibration mode $\bar{\mathbf{u}}^{[r]}$ was given with the first natural vibration mode, excluding the six rigid body modes, on the bottom plane boundary in the reference model shown in Fig. 6a, i.e.

$$\Gamma_D = \{\mathbf{x} \in \Gamma |\, x_2 = 0\}\,, \tag{34}$$

$$\bar{\mathbf{u}}^{[r]} = \left\{ u_2^{[1]} \in H^{1/2}(\Gamma_D) \middle|\; u_2^{[1]} \text{ at Fig. 6a} \right\}. \tag{35}$$

In the analysis of domain variation by the traction method, the bottom plane boundary was completely fixed and all the side plane boundaries were fixed in the normal direction, i.e.

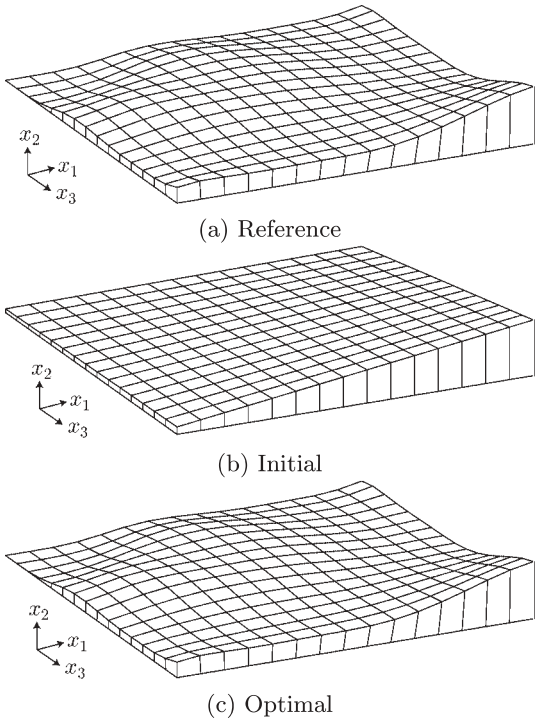

Fig. 6 Plate-like continuum problem: shape optimization of three-dimensional free supported plate-like continuum in which the first natural vibration mode on the bottom plane, $\mathbf{u}^{[1]}$, approaches the first natural vibration mode on the bottom plane, $\bar{\mathbf{u}}^{[1]}$, of the reference plate-like continuum shown in (a)

$$D = \Big\{ \mathbf{V} \in \left(H^1(\Omega)\right)^3 \Big| \ \mathbf{V}|_{\{\mathbf{x}\in\Gamma | x_2=0\}} = 0\,, \text{ fixing normal direction on all the side plane} \Big\}\,. \tag{36}$$

The lower limit of the first natural vibration eigenvalue $\bar{\lambda}^{[1]}$ and the upper limit of the volume $\bar{M}$ were chosen as $\lambda^{[1]}$ and $\int_\Omega \mathrm{d}x$ for the reference model shown in Fig. 6a. Starting from the initial model shown in Fig. 6b, the convergent optimal model was obtained as shown in Fig. 6c.

Figure 7 illustrates the iteration history of the objective functional of the squared error integral $E(\alpha\mathbf{u}^{[1]} - \bar{\mathbf{u}}^{[1]}, \alpha\mathbf{u}^{[1]} - \bar{\mathbf{u}}^{[1]})$, the first natural vibration eigenvalue $\lambda^{[1]}$, and the volume $\int_\Omega \mathrm{d}x$, which were successfully converged to the optimal condition satisfying the inequality constraints on $\lambda^{[1]}$ and $\int_\Omega \mathrm{d}x$. The natural vibration eigenvalue $\lambda^{[1]}$ increased with the shape change in this problem. A comparison of the first natural vibration modes $\alpha\mathbf{u}^{[1]}$ of the reference, initial, and optimal plate-like continua with the optimal α determined by (15) in the bottom plane boundary is illustrated with a bird's-eye view in Fig. 8 and the specified view on the bottom line A–B shown in Fig. 8 is illustrated in Fig. 9. From the results, it can be confirmed that the first natural vibration mode approached the prescribed mode uniformly.

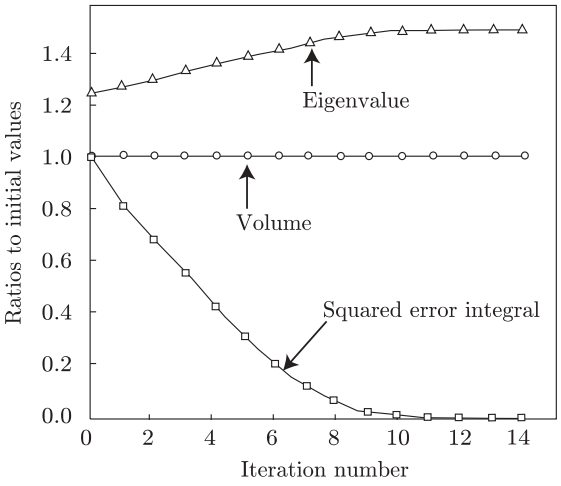

Fig. 7 Plate-like continuum problem: iteration history of the objective functional of the squared error integral $E(\alpha\mathbf{u}^{[1]} - \bar{\mathbf{u}}^{[1]}, \alpha\mathbf{u}^{[1]} - \bar{\mathbf{u}}^{[1]})$, the first natural vibration eigenvalue $\lambda^{[1]}$, and the volume $\int_\Omega \mathrm{d}x$

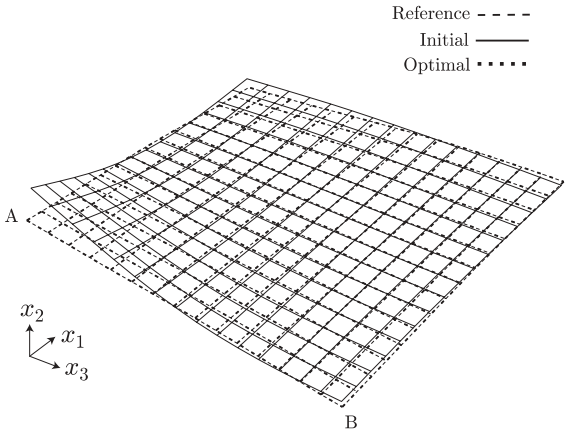

Fig. 8 Plate-like continuum problem: comparison of the first natural vibration modes $\alpha\mathbf{u}^{[1]}$ of the reference, initial, and optimal beam-like continua with the optimal α determined by (15) on the bottom plane

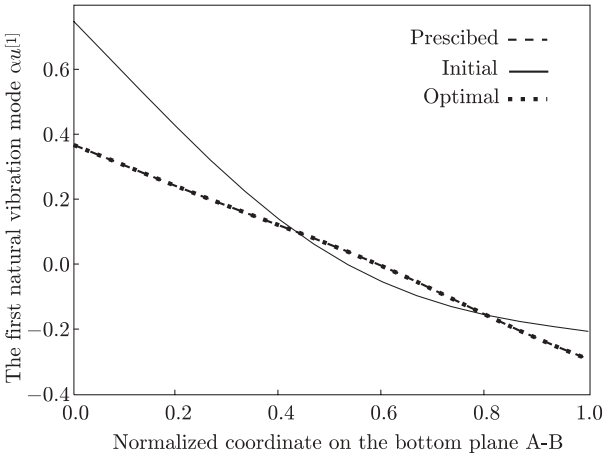

Fig. 9 Plate-like continuum problem: comparison of the first natural vibration modes $\alpha\mathbf{u}^{[1]}$ of the reference, initial, and optimal beam-like continua with the optimal α determined by (15) on A–B of the bottom plane shown in Fig. 8

7 Conclusion

This paper presented a method for solving boundary shape optimization problems of linear elastic continua in which vibration mode shapes approach prescribed vibration mode shapes on specified sub-boundaries by applying the traction method. The shape optimization problem was formulated as the minimization of the integral of the squared error of an assigned natural vibration mode shape from a prescribed mode shape on the specified sub-boundary under inequality constraints on the assigned natural vibration eigenvalue and the volume. The fundamental relations for the shape gradient of the problem were derived by the adjoint variable method, the Lagrange multiplier method, and the formula for the material derivative. The solution for the adjoint equation was presented by using modal coordinate system. The results of the numerical analyses verified that the traction method with the shape gradient performed properly.

The demonstrated problems consisted of 3×50 and 16×16 design variables for the beam-like continuum and the plate-like continuum problems respectively. It is not easy to apply the parametric optimization techniques presented by Fox and Kapoor (1968), Nelson (1976), Wang (1991), Hagiwara and Ma (1994), and Lin and Lim (1995) to these problems because of the number of design

variables. The presented results show the superiority of the presented method in terms of consumption of CPU time.

References

Allemang, R.J.; Brown, D.L. 1982: A correlation coefficient for modal vector analysis. In: *Proceedings of 1st International Modal Analysis Conference*, pp. 110–116. Orlando, New York: Union College

Azegami, H. 2000: Solution to boundary shape identification problems in elliptic boundary value problems using shape derivatives. In: Tanaka, M.; Dulikravich, G.S. (eds.) *Inverse Problems in Engineering Mechanics II*, pp. 277–284. Tokyo: Elsevier

Azegami, H.; Kaizu, S.; Shimoda, M.; Katamine, E. 1997: Irregularity of shape optimization problems and an improvement technique. In: Hernandez, S.; Brebbia, C.A. (eds.) *Computer Aided Optimization Design of Structures V*, pp. 309–326. Southampton: Computational Mechanics Publications

Azegami, H.; Shimoda, M.; Katamine, E.; Wu, Z.C. 1995: A domain optimization technique for elliptic boundary value problems. In: Hernandez, S.; El-Sayed, M.; Brebbia C.A. (eds.) *Computer Aided Optimization Design of Structures IV, Structural Optimization*, pp. 51–58. Southampton: Computational Mechanics Publications

Azegami, H.; Wu, Z.C. 1996: Domain optimization analysis in linear elastic problems: approach using traction method. *JSME Int. J. Ser. A* **39**, 272–278

Bendsoe, M.P.; Kikuchi, N. 1988: Generating optimal topologies in structural design using a homegenization method. *Comput. Methods Appl. Mech. Eng.* **71**, 197–224

Diaz, A.; Kikuchi, N. 1992: Solutions to shape and topology eigenvalue optimization problems using a homegenization method. *Int. J. Numer. Methods Eng.* **35**, 1487–1502

Fox, R.L.; Kapoor, M.P. 1968: Rate of change of eigenvalues and eigenvector. *AAIA J.* **6**, 2426–2429

Hagiwara, I.; Ma, Z.D. 1994: A new mode-superposition technique for truncating lower- and/or higher-frequency modes (application of eigenmode sensitivity analysis). *JSME Int. J. Ser. C* **37**, 14–20

Hagiwara, I.; Tsuda, M.; Fujiwara, T.; Nakamura, K. 1987: Optimization analyses for body structure using stiffness and eigenmode sensitivity analysis methods. *Trans. SAE* **35**, 81–87 (in Japanese)

Lin, R.M.; Lim, M.K. 1995: Eigenvector derivatives of structures with rigid body modes. *AAIA J.* **34**, 1083–1085

Ma, D.Z.; Cheng, H.C.; Kikuchi, N. 1994: Structural design for obtaining desires eigenfrequencies by using the topology and shape optimization method. *Comput. Syst. Eng.* **51**, 77–89

Nelson, R.B. 1976: Simplified calculation of eigenvector derivatives. *AAIA J.* **14**, 1201–1205

Pironneau, O. 1984: *Optimal Shape Design for Elliptic Systems*. New York: Springer-Verlag

Shimoda, M.; Azegami, H.; Sakurai, T. 1998: Traction method approach to optimal shape design problems. *SAE 1997 Trans., J. Passenger Cars* **106**, 2355–2365

Sokolowski, J.; Zolésio, J.P. 1991: *Introduction to Shape Optimization: Shape Sensitivity Analysis*. New York: Springer-Verlag

Tenek, L.H.; Hagiwara, I. 1994: Eigenfrequency maximization of plates by optimization of topology using homegenization and mathematical programming. *JSME Int. J. Ser. C* **37**, 667–677

Wang, B.P. 1991: Improved approximate methods for computing eigenvector derivatives in structural dynamics. *AAIA J.* **29**, 1018–1020

Wu, Z.C.; Azegami, H. 1995a: Domain optimization analysis in natural vibration problems: approach using traction method. *Trans. JSME Ser. C* **61**, 930–937 (in Japanese)

Wu, Z.C.; Azegami, H. 1995b: Domain optimization analysis in natural vibration problems: mass minimization problems. *Trans. JSME Ser. C* **61**, 2691–2696 (in Japanese)

Wu, Z.C.; Azegami, H. 1995c: Domain optimization analysis in frequency response problems: approach using traction method. *Trans. JSME Ser. C* **61**, 3968–3975 (in Japanese)

Wu, Z.C.; Sogabe, Y.; Arimitsu, T.; Azegami, H. 1999: Shape optimization analysis of transient and random vibration problems. In: Gu, Y.X.; Duan, B.Y.; Azegami, H.; Kwak, E.M. (eds.) *Proceedings of the First China-Japan-Korea Joint Symposium on Optimization of Structural and Mechanical Systems*, pp. 101–108. Xian: Xidian University Press

Wu, Z.C.; Sogabe, Y.; Arimitsu, T.; Azegami, H. 2000: Shape optimization of transient response problems. In: Tanaka, M.; Dulikravich, G.S. (eds.) *Inverse Problems in Engineering Mechanics II*. Tokyo: Elsevier

Wu, Z.C.; Sogabe, Y.; Azegami, H. 1997: Shape optimization analysis for frequency response problems of solids with proportional viscous damping. *Key Eng. Mater.* 145–149, 172–178

Zolésio, J.P. 1981: The material derivative (or speed) method for shape optimization. In: Haug, E.J.; Cea, J. (eds.) *Optimization of Distributed Parameter Structures*, Vol. 2, pp. 1089–1151. Alphen aan den Rijn: Sijthoff & Noordhoff